

# Structural, linear and nonlinear optical properties of multicomponent bulk and thin film tellurite glass

S. KUMARI<sup>a,\*</sup>, S. YADAV<sup>b</sup>, D. MOHAN<sup>a</sup>

<sup>a</sup>Dept. of Physics, G. J. U. S. & T. Hisar-125001, Haryana, India

<sup>b</sup>Dept of Physics, Baba Mastnath University Asthal Bohar, Rohtak-124001, Haryana, India

The conventional melt quench technique was used to synthesize the bulk glass of composition  $60\text{TeO}_2.12\text{Bi}_2\text{O}_3.18\text{B}_2\text{O}_3.10\text{ZnO}$ , and the thin film was deposited by thermal evaporation technique. X-ray diffraction pattern reveals the amorphous nature of the material under study. The direct bandgap of as-deposited thin films and bulk glass has been calculated using Tauc's Plot and found to be 3.0 eV and 2.81 eV, respectively. Nonlinear optical parameters of bulk and thin-film glasses have been estimated using semi-empirical relations. Nonlinear optical susceptibility has found to be  $1.272 \times 10^{-13}$  esu (bulk) and  $1.810 \times 10^{-13}$  esu (thin film), respectively. The nonlinear refractive index has been estimated for both bulk ( $2.733 \times 10^{-12}$ ) and thin-film ( $3.773 \times 10^{-12}$ ). The high nonlinearity of the thin-film is useful as potential applications in optoelectronic devices.

(Received February 18, 2020; accepted December 7, 2020)

**Keywords:** Nonlinear refractive index, Third order nonlinear susceptibility, Thermal evaporation

## 1. Introduction

Among today's dynamic research topics optical communication has drawn much attention because of the innovations it contributed to scientific and technological applications. It transmits larger amount of information at lower costs for longer distances as compared to that transmitted by classic transmission media such as copper wires or radio waves. Glasses are best media for development of optical communication system due to their promising properties [1]. During the past few decades  $\text{TeO}_2$  based glasses have been focus of vast research efforts for optical communication systems due to their transparency in visible and near infrared region (0.4 to 6  $\mu\text{m}$ ) and high values of index of refraction ( $n \geq 2$ ) that supports the fabrication of waveguides as well as fibres with strong light confinement [2]. However, it is difficult to synthesize pure  $\text{TeO}_2$  glass because it has tendency to devitrify. Thus it necessitates the addition of other oxides not only for the stabilization of glass structure but also for the improvement of optical properties of glass. The glass composition having heavy metal oxides such as  $\text{Bi}_2\text{O}_3$ ,  $\text{Nb}_2\text{O}_5$  etc. exhibit various significant optical features like high transmission in near IR region, high value of refractive index and optical nonlinearity [3].

Recently, to achieve the high value of refractive index multicomponent oxide glasses have been developed. Generally, the glass with large value of refractive index exhibits colouring because of the optical absorption edge that is located in the near visible wavelength not in the deep UV. The transmission spectra of high refractive index glass get deteriorated around the absorption edge, therefore these glasses show greyish or yellowish colour. This type of deterioration near absorption edge may happen not only due to the contaminated impurities [4] but also due to the disorder in the glass structure [4,5]. The

index of refraction as well as optical nonlinearity is enhanced significantly in the vicinity of the absorption edge by the electronic resonance [4].

The incorporation of heavy metal oxide like  $\text{Bi}_2\text{O}_3$  into tellurite glass leads to possess large polarizability, high value of refractive index, high optical basicity and large optical susceptibility [6,7]. Now days, there is restriction on lead oxide glasses in different industries as these are hazardous to environment. In this context  $\text{Bi}_2\text{O}_3$  is considered as the best substitute of lead oxide as it exhibits significant properties such as wide transmission range, low value of melting temperature, high value of refractive index and non-toxicity [3].

Also the incorporation of boric acid into tellurite glasses enhances the glass forming ability and transparency of glass. It has strong B-O bonding and can exist in both 3 as well as 4 co-ordinated environments. Thus it can form the glass with high thermal stability, good rare earth ion solubility, good transparency and good chemical durability. Moreover, the addition of ZnO to the glassy matrix decreases the rate of crystallization in it [6].

In many practical applications of these materials, one requires thin film glasses with fine optical quality. These thin film glasses were synthesized by various researchers using thermal vapour deposition, sol-gel, and sputtering or pulse laser deposition but still it is a challenge to produce smooth thin film glasses with desired optical quality [8-12]. The present work focuses on the deposition of thin film tellurite glasses by thermal evaporation having large values of nonlinear index of refraction. Also the comparison of linear and nonlinear optical responses of bulk glasses and as-deposited thin film glass have been done and observed differences have been discussed.

## 2. Sample preparation and experimental technique

Glass samples having composition  $60\text{TeO}_2.12\text{Bi}_2\text{O}_3.18\text{B}_2\text{O}_3.10\text{ZnO}$  were synthesized by rapid melt quenching method that include the mixing of high purity AR reagent  $\text{TeO}_2$ ,  $\text{Bi}_2\text{O}_3$ ,  $\text{H}_3\text{BO}_3$  and  $\text{ZnO}$  as the starting materials. 20g of as-stated composition has been mixed thoroughly in an agate mortar-pestle. After that mixed oxides were melted in a porcelain crucible at temperature  $800^\circ\text{C}$  in an electric furnace for about 30 minute. The melt was stirred regularly to maintain the homogeneity and proper mixing. After the completion of melting process, the molten liquid was poured onto a stainless steel plate and pressed quickly by another one at room temperature.

The glass sample synthesized by above method was then ground in an agate mortar pestle to form a homogeneous mixture for deposition of thin films. The thin film glass was deposited on glass substrate using thermal evaporation technique. The initial substrate was cleaned ultrasonically using ethanol, acetone and distilled water each for 15 minute. The powdered glass was evaporated in vacuum chamber at pressure of  $4 \times 10^{-6}$  mbar in the thermal coating unit. As the film was deposited under non equilibrium conditions, a further heat treatment was required. For this the film has annealed in ambient air at a temperature of  $420^\circ \pm 30^\circ$ . The heating and cooling rates were decided under the vitrification conditions. The compositional analysis was carried out using energy dispersive X-ray analysis (EDX) using Merlin Compact from Carl Zeiss, Germany. The thickness of thin film was measured using profilometer (MarSurf LD 260 Y from Mahar GmbH) and Tauc's plot was used to determine the optical band gap of the samples.

## 3. Results and discussion

### 3.1. Structural and compositional analysis

X-ray diffraction is considered as a useful tool to confirm the nature of any material.

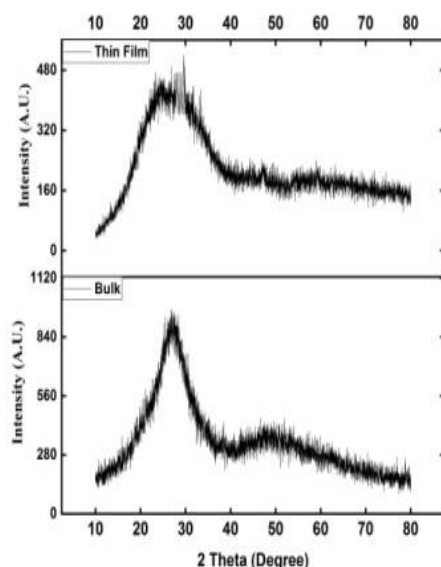


Fig. 1. X-ray Diffractogram of  $60\text{TeO}_2.12\text{Bi}_2\text{O}_3.18\text{B}_2\text{O}_3.10\text{ZnO}$  bulk glass and thin-film glass

The diffractograms of bulk as well as thin-film glass recorded by X-ray diffractometer (Miniflex-II) from  $10^\circ$  to  $80^\circ$  as shown in Fig. 1. A long-range structural disorder by showing broad diffuse scattering at lower Bragg angles, i.e.,  $25^\circ$  to  $30^\circ$ , indicates the amorphous nature of samples. For present tellurite glass composition diffused peak is found around  $28^\circ$ .

EDX of the thin-film glass shown in Fig. 2 that confirms the presence of all the components like tellurium, bismuth, zinc, and boron in the composition. EDX verifies that all elements are present in the host matrix.

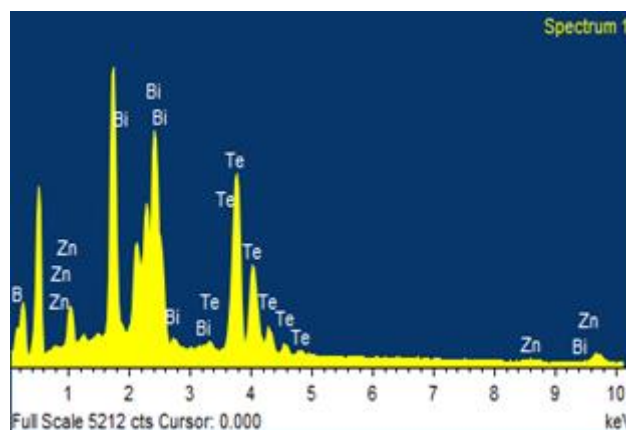


Fig. 2. EDX spectrum of thin-film glass (color online)

### 3.2. Optical analysis

In crystalline and amorphous materials, the electronic band structure and optical transitions can be investigated by the study of optical absorption. The UV-visible absorption spectra of as stated glasses have been recorded in the wavelength range 300-1000 nm by using a double beam UV Infrared spectrophotometer. The relative rate of decrease in the intensity of light along its path of propagation can be determined by linear absorption coefficient which is given as [13].

$$\alpha(\nu) = \frac{\text{Absorbance}}{\text{thickness of sample}}$$

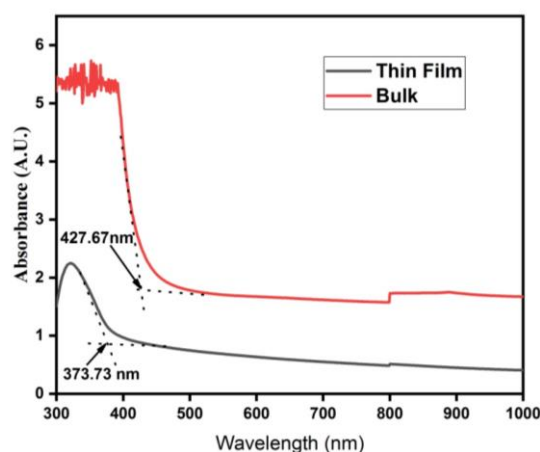


Fig. 3. Absorption spectra of bulk and thin-film glass (color online)

Fig. 3 depicts the absorption spectra of present glass samples. The cut off wavelength of the samples was determined and observed that there is a blue shift in the absorption edge on moving from bulk to thin-film glass from 427.67 nm to 373.73 nm, which may be because of structural rearrangement of glass network and modifier [13]. It is worth noting that the absorption coefficient of non-crystalline semiconductor in the region of high

absorption ( $\alpha \geq 10^4 \text{ cm}^{-1}$ ) is determined by Tauc's relation [14].

$$(\alpha h\nu)^n = B(h\nu - E_g) \quad (1)$$

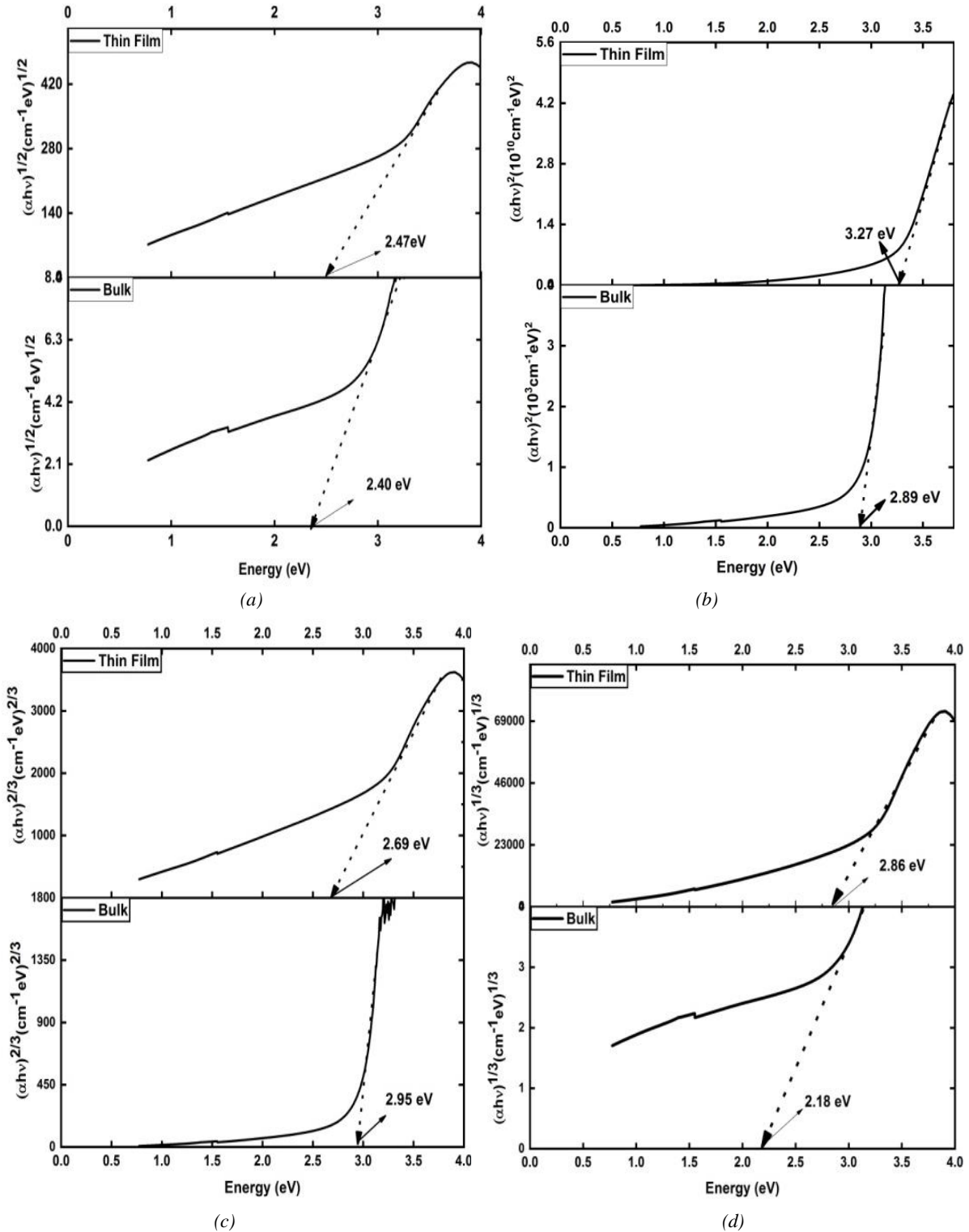


Fig. 4. Variation of  $(\alpha h\nu)^n$  against photon energy  $h\nu$  for (a)  $n = 2$  (b)  $n = 1/2$ , (c)  $n = 1/3$  and (d)  $n = 2/3$  for the glass system

Here  $B$  is a constant that depends on refractive index and effective mass of charge carriers. Also  $E_g^{opt}$  is defined as the optical band gap that according to Mott and Davis [15] is located between localized states in the vicinity of mobility edge and  $h\nu$  is the incident photon energy. The different values of exponent  $n$  viz.  $1/2$ ,  $2$ ,  $1/3$ , and  $2/3$  correspond to indirect allowed, direct allowed, indirect forbidden and direct forbidden transitions, respectively [14].

As the optical band gap values so obtained vary according to the selection of value of exponent  $n$  so it could not be decided really which value of  $n$  should be selected for better results? Therefore, only the type of conduction mechanism may be determined by Eq. (1) and one another parameter that is imaginary part of dielectric constant  $\epsilon_i$  can be used for determining  $E_g$  as well as exact value of exponent  $n$ .

The optical band gap of the samples has been determined by extrapolating the linear region of curves in such a manner to meet the  $h\nu$  axis where the condition

$\alpha h\nu = 0$  is satisfied and the values so determined for different values of  $n$  are tabularized in Table 1 and shown in Fig. 4(a), (b), (c) and (d).

The higher value of  $E_g$  for thin-film glass as compared to that of bulk glass may express in terms of confinement. In the bulk glass, the energy levels corresponding to a large number of atoms or molecules merge to form a group of adjoining energy levels called bands. In the case of a thin film, size reaches nano-scale, there exist less number of atoms or molecules. Therefore decrease in the overlapping of the energy levels will result in the narrow width of bands.

Thus higher the optical band gap more restricted is the movement of electrons, and hence there is a shift in the absorption edge towards lower wavelength.

### 3.3. Determination of refractive index

The optical properties of glass are governed by complex dielectric constant as well as index of refraction.

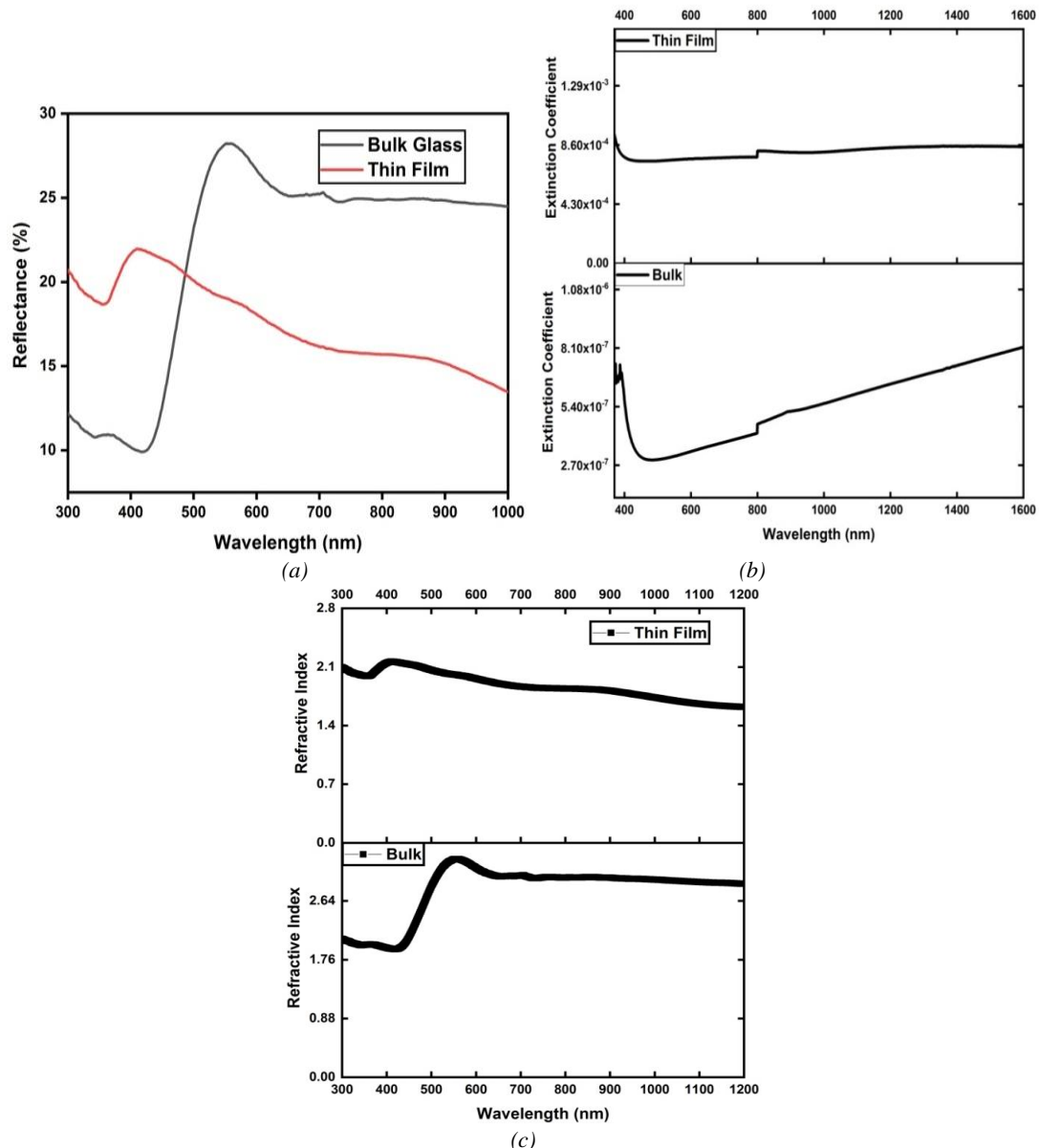


Fig. 5. Variation of (a) reflectance (b) extinction coefficient, (c) refractive index with wavelength (color online)

Both components can be determined using an optical reflectance graph of glass. Hence the value of  $n$  as well as  $k$  given as

$$n = \frac{1+R}{1-R} + \sqrt{\frac{4R}{(1-R)^2} - k^2} \quad \text{and} \quad k = \frac{\alpha\lambda}{4\pi} \quad \text{for bulk [16]}$$

$$\text{For thin films [17] value of } n = \frac{1+R+\sqrt{R}}{1-R}$$

Here  $R$  stands for the reflectivity of glass samples in a transparent region. The change in reflectance, index of refraction and extinction coefficient as a function of wavelength are shown in Fig. 5(a), (b), and (c), respectively.

The values of refractive indices so obtained are listed in Table 1. The bulk glass possesses higher value of the refractive index as compared to that of thin-film glass. The smaller value of the refractive index of film glass could be due to the variation in composition in thin films. This may be because of the higher density of bulk glass in comparison with thin-film glass due to higher porosity degree of thin film in accordance with Lorentz-Lorentz equation that gives a direct proportion between refractive index and density of the material [2].

An anomalous dispersion is observed in bulk (in the wavelength range 300-750 nm) and thin-film glass (in wavelength range 300-450nm) that can be explained in terms of the multi-oscillator model. Beyond the above region, normal dispersion is observed, which can be analyzed using Wemple and Di Domenico single oscillator model [18,19]. According to WDD model there is a relation between  $n$  and  $h\nu$ , i.e.

$$(n^2 - 1)^{-1} = \frac{E_o}{E_d} - \frac{1}{E_o E_d} (h\nu)^2 \quad (2)$$

where  $E_d$  and  $E_o$  correspond to dispersion energy and the effective oscillator energy, respectively, the dispersion energy gives an idea of how strong are interband optical transitions. Also, the bond energy of chemical bonds of the glass is determined from the effective oscillator energy  $E_o$ . In the plot of  $1/(n^2-1)$  versus  $E^2$  as shown in Fig. 6, a straight line fitting has been done. The intercept  $E_o/E_d$  with ordinate axis and slope  $(E_o E_d)^{-1}$  of the linear portion of the plot are used to determine the value of  $E_o$  and  $E_d$ . The values so evaluated are listed in table 1 for bulk and thin-film glass. Thin-film glass has a higher value of  $E_o$  than that of bulk glass, which may be due to the higher bond energy of the covalent bond present in the thin-film glass.

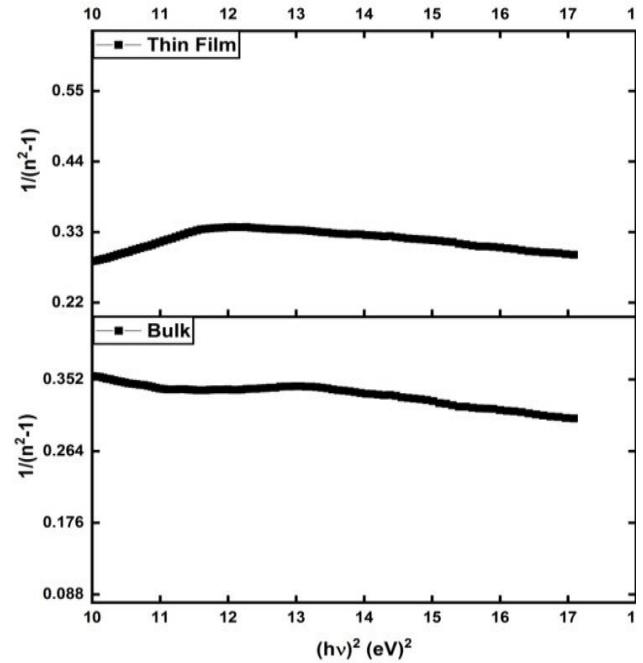


Fig. 6. Variation of  $(n^2-1)^{-1}$  with  $(h\nu)^2$  for bulk and thin film glass

### 3.4. Dielectric constant

The dielectric constant gives the idea of how the structure of a solid is related to the electronic transition between bands. So one can deduce useful information from the dielectric spectra about the band structure of a material in solid form. The following relations can be used to determine the real and imaginary part of dielectric constant ( $\epsilon_r$ ,  $\epsilon_i$ ) [10].

$$\epsilon_r = n^2 - k^2 \quad (3)$$

$$\epsilon_i = 2nk \quad (4)$$

The variation of  $\epsilon_i$  versus photon energy is shown in Fig. 7 for as studied glass samples. The imaginary part of the dielectric constant is related to the extinction coefficient, which is also related to the absorption of light. The optical band gap can be evaluated by extrapolating  $\epsilon_i$  to zero. The value of energy gap so obtained are in good agreement with the values calculated from absorption spectra for direct allowed transition for bulk as well as thin-film glass.

Table 1. Optical band gap, dispersion energy, effective oscillator energy, static refractive index, nonlinear optical susceptibility and nonlinear refractive index of 60TeO2.12Bi2O3.18B2O3.10ZnO bulk and thin film glass

Parameters	Bulk Glass	Thin film
$E_g$ (eV)	2.81	3.0
$E_d$ (eV)	14.11	16.45
$E_o$ (eV)	6.79	7.25
$\chi^{(3)} \times 10^{-13}$ esu	1.272	1.810
$n_2 \times 10^{-12}$ esu	2.733	3.773

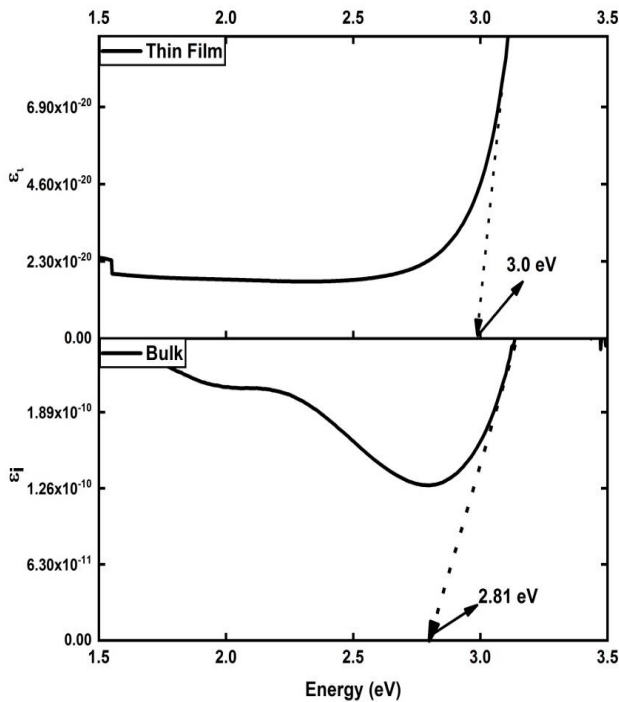


Fig. 7. Variation of imaginary part of dielectric constant with respect to photon energy

### 3.5. Nonlinear optical properties

Nonlinear optics describes the nonlinear polarization behaviour of the material with the incidence of highly intense radiation. The fabrication of essential components of integrated photonics like optical switching and frequency conversion devices necessitates the estimation of various nonlinear optical parameters like nonlinear refractive index and third-order nonlinear optical susceptibility of the material to be used. The nonlinear optical susceptibility and nonlinear refractive index approximated by applying the model proposed by Tichy et al. [20] where generalized Miller's rule [21] and static refractive index calculated from WDD single oscillator model [18] are combined

$$\gamma^{(3)} = \frac{A}{(4\pi)^4} \left( \frac{E_d}{E_o} \right)^4 \quad (5)$$

and

$$n_2 = \frac{12\pi\chi^{(3)}}{n_o} \quad (6)$$

where A is a constant having approximate value of  $1.7 \times 10^{-10}$  esu.

The nonlinear optical susceptibility and nonlinear refractive index of bulk, as well as thin-film glass obtained by using Eq. (5) and (6) are listed in Table 1. The estimated values of the samples show good agreement with the values reported in literature [2]. Table 1 also predicts that thin-film glass owns higher magnitudes of optical nonlinearity as compared to bulk glass.

## 4. Conclusions

The quaternary tellurite glass system in bulk, as well as thin-film form, have been developed successfully using the melt quench technique and thermal evaporation method, respectively. Their non-crystalline nature has been ascertained using the X-ray diffraction method. The composition of the thin film has been confirmed using EDAX. Thin-film glass possesses a higher optical band gap (3.0 eV) as compared to bulk glass (2.81 eV), which is due to the confinement effect. Nonlinear optical susceptibility has found to be  $1.272 \times 10^{-13}$  esu (bulk) and  $1.810 \times 10^{-13}$  esu (thin film), respectively. The nonlinear refractive index has been estimated  $2.733 \times 10^{-12}$  esu (bulk) and  $3.773 \times 10^{-12}$  esu (thin film). Higher magnitude of nonlinear optical susceptibility and nonlinear refractive index of thin-film glass than that of bulk glass make it a potential candidate for nonlinear applications.

## References

- [1] A. E. Ersundu, M. Celikbilek, S. Aydın, A review of scanning electron microscopy investigations in tellurite glass systems, in: A. Mendez-Vilas (Ed.), Formatex, 1105 (2012).
- [2] D. Munoz-Martin, H. Fernandez, J. M. Fernandez-Navarro, J. Gonzalo, J. Solis, J. Appl. Phys. **104**, 113510 (2008).
- [3] M. I. Sayyed, Journal of Alloys and Compounds **688**, 111 (2016).
- [4] T. Hasegawa, Journal of Non-Crystalline Solids **357**, 2857 (2011).
- [5] V. I. Arbutov, Glass Phys. Chem. **22**, 477 (1996).
- [6] V. Dimitrov, T. Komatsu, J. Non-Cryst. Solids **249**, 160 (1999).
- [7] P. Yasaka, N. Pattanaboonmee, H. J. Kim, P. Limkitjaroenporn, J. Kaewkhao, Ann. Nucl. Energy **68**, 4 (2014).
- [8] L. Weng, S. N. B. Hodgson, J. Non-Cryst. Solids **297**, 18 (2002).
- [9] E. B. Intyushin, I. Yu. Chigirinskii, Glass Physics and Chemistry **31**(2), 162 (2005).

- [10] A. M. Emara, M. M. Makhlof, E. L. Sayed Yousef, *Journal of Non-Crystalline Solids* **515**, 58 (2019).
- [11] H. Kong, J. B. Yeo, H.Y. Lee, *Journal of the Korean Physical Society* **66**, 1744 (2015).
- [12] E. B. Intyushin, V. A. Novikov, *Thin Solid Films* **516**, 4194 (2008).
- [13] R. S. Kundu S. Dhankhar, R. Punia, K. Nanda, N. Kishore, *Journal of Alloys and Compounds* **587**, 66 (2014).
- [14] J. Tauc *Amorphous and Liquid Semiconductors*, Plenum Press, New York, (1974).
- [15] N. F. Mott, E. A. Davis, *Electronic Processes in Non-Crystalline Materials*, Clarendon Press, Oxford, 389 (1971).
- [16] A. A. Ali, H. M. Shaaban, A. Abdallah, *J. Mater. Res. Technol.* **7**(3), 240 (2018)
- [17] F. Padera. UV/Vis Spectroscopy. [http://www.perkinelmer.ca/CMSResources/Images/44-153901APP\\_Thin-films.pdf](http://www.perkinelmer.ca/CMSResources/Images/44-153901APP_Thin-films.pdf), 2013. [Online; accessed 11-Nov-2019].
- [18] S. H. Wemple, M. Jr. Didomenico, *Phys. Rev. B* **3**, 1338 (1971).
- [19] S. H. Wemple, *Phys. Rev B* **7-8**, 3767 (1973).
- [20] L. Tichy, H. Ticha, K. Handlr, *J. Mater. Sci.* **23**, 229 (1988).
- [21] J. Wyne, *J. Phys. Rev.* **178**, 1295 (1969).

---

\* Corresponding author: sonialuhach24@gmail.com